Influence of Binding Interface between Active and Support Layers in Composite PDMS Membranes on Permeation Performance

Er Shi, Weixing Huang, Zeyi Xiao, Donghuai Li, Ming Tang

School of Chemical Engineering, Sichuan University, Chengdu 610065, China

Received 11 April 2006; accepted 5 June 2006
DOI 10.1002/app.25358
Published online in Wiley InterScience (www.interscience.wiley.com).

ABSTRACT: Effect of the binding interfaces of composite polydimethylsiloxane (PDMS) membranes on their pervaporation performance was studied. The membranes were made up of PDMS as active skin layer and polysulfone (PSF) or polyamide (PA) as supporting layer. PDMS-PSF membrane was numbered 1, and PDMS-PA membrane numbered 2. The pervaporation experiments were carried out by using the composite membranes and dilute ethanol–water mixture. The experimental measurements for the permeation performance under various operating conditions (e.g., feed concentration and temperature) showed that the specific permeation rate of membrane 2 was over membrane 1 by seven times at least. A resistance-in-series model was applied to formularize the transport of the permeants. Influence of the binding interfaces between the active skin layer and support layers in these membranes on pervaporation performance was analyzed. The cross section morphology of the membranes and chemical element distribution along membrane thickness were examined by using SEM and EDS. It was found that, although the PDMS intrusion layer into PSF near the interface was only about 2 μm, it gave significant effect on the permeation performance. It implied that the resistance produced by the intrusion layer into PSF was apparently larger than that of PDMS intruding PA and over intrinsic PDMS resistance. These should be probably attributed to structures and formation of the binding interfaces. J Appl Polym Sci 104: 2468–2477, 2007

Key words: composite PDMS membrane; permeation; binding interface; pervaporation; transport resistance

INTRODUCTION

Pervaporation has been considered as an alternative method for separation of organic liquid mixtures, especially dilute ethanol–water systems, since the vapor–liquid equilibrium can be altered by the perm-selective membranes.[1,2] Many organophilic polymeric materials have been reported to be good candidates of the membranes for ethanol–water separation. Polydimethyl-siloxane (PDMS) polymer is among those.[3,4] But from a critical thickness outward, PDMS presents poor mechanical and film-forming abilities.[5] These disadvantages have been overcome by using the composite multilayer structure, in which PDMS as the active skin layer is plated on a porous polymeric support by various technologies.[6–9] The mass transfer through the composite membrane has become a challenging problem.

Correspondence to: Z. Xiao (zeyix@hotmail.com or xzy_98@yahoo.com or mgch@peoplemail.com.cn).

Contract grant sponsor: National Natural Science Foundation of China; contract grant numbers: 20176030, 20276041.

Although the resistance of the support in the case of a composite membrane is not yet really well understood, its importance has been demonstrated for a number of systems.[10,11] The perm-selective performance of a composite membrane is mostly depended upon the top active skin layer, but also associated with the support layer to some extent. First, the porosity of the support layer should be as high as possible to decrease the resistance for the permeation species flowing through the capillaries in the support. On the other hand, the top layer material intruding into the pores of the support must be well controlled to avoid new and unexpected large mass transfer resistance in addition to those of the top layer and the support layer. Some researchers have previously studied and modeled the effect of intrusion of top layer in porous support. Henis and Tripodi[12] developed a resistance model, in which the top PDMS layer resistance was in series with a parallel resistance of the PDMS-filling pores and solid polysulfone bulk for the sublayer, to describe the behavior of the dense layer and calculate the gas permeation properties of a composite membrane. Vankelecom et al.[9] studied the effect of intrusion of PDMS in Zirfon® (polysulfone-filled zirconium oxide) support layers on pervaporation for the aqueous

ethanol system. With different pretreatments for the support layer, it was observed that the normalized fluxes of the composite membrane depended upon the pore structure intactness and the intrusion of PDMS. Lipnizki et al.[13] analyzed the resistance of the binding interface and focused on the influence of the support layer on diffusion path and the driving force. Few researchers have been building a bridge between modeling of support layer and binding interface and the experimental data for those.

In this study, a composite PDMS membrane with polyamide (PA) supporting layer has been prepared in our laboratory, which was of very high permeability and moderate selectivity, compared with similar composite membranes reported in literatures. With the prepared membrane and a commercial composite PDMS membrane offered by a company, characterization of the membranes and pervaporation tests for ethanol–water solution were accomplished. Based on resistance-in-series model, the intensive analysis was conducted to exploit the transport resistances and their structure–dependence of these two membranes. As focus of this work, influence of binding interfaces between the active layer and support layers in these PDMS composite on permeation performance was explored and some interesting behaviors were found.

MODEL OF COMPOSITE MEMBRANES FOR PERVAPORATION

In this study, we consider the behavior of two composite membranes. A schematic representation of cross section of them is illustrated in Figure 1.

According to the resistance-in-series model, the transport of species through the composite consists of the following consecutive processes: diffusing through the liquid boundary layer to the membrane surface; dissolving into the dense PDMS layer; diffusing through the dense layer; being desorbed out of the dense layer as vapor, and flowing or diffusing in capillaries of the support.[14] Hence, the overall resistance to the mass transfer for a component can be expressed as:

$$\frac{1}{k_{\mathrm{ov}}} = \frac{1}{k_l} + \frac{\delta}{P} + \frac{\delta_v}{D_v} \tag{1}$$

where k_{ov} and k_l is the overall mass transfer coefficient and liquid film mass transfer coefficient, respectively; D_v is permeability (or equivalent diffusion coefficient) through the support layer; P, the liquid permeability of dense layer, δ and δ_v, thickness of the dense layer and the support layer, respectively.

In the case of a nonporous composite membrane [as Fig. 1(a)], the resistance of dense layer is defined

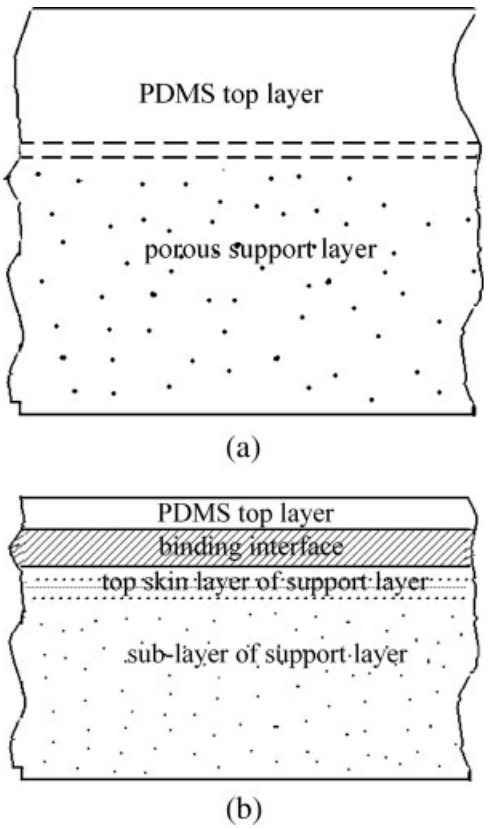

Figure 1 Structure of model composite membranes of PDMS with porous support.

by one overall resistance,[15] which efficiently combines the two resistances of the PDMS top layer and binding interface.

$$\frac{P}{\delta} = \left(\frac{\delta_m}{P_m} + \frac{\delta_{\mathrm{binding}}}{P_{\mathrm{binding}}}\right)^{-1} \tag{2}$$

When a physical change is considered between the PDMS and polysulfone in the binding layer, vapor permeability coefficient P/δ is expressed as a series-resistance plus a parallel-resistance by several authors:[12,13,16]

$$\frac{P}{\delta} = \left(\frac{\delta_m}{P_m} + \frac{\delta_{\mathrm{binding}}}{P_m\varepsilon_s + P_{\mathrm{support}t}(1-\varepsilon_s)}\right)^{-1} \tag{3}$$

where P_{binding}, P_m, and P_{support} represents liquid permeability of binding interface, PDMS top layer, and support material, respectively. ε_s is surface porosity of microporous support. Where there is no binding interface, the second term in the right of eq. (3) is zero.

A support layer is usually a microporous or ultrafiltration membrane with an average pore size <1 μm. The mass transport through the porous support should be controlled by either Knudsen diffusion or

viscous flow. Thus, $D_{i,v}$ can be estimated by a combination of Knudsen diffusion and viscous flow:[17]

$$D_{i,v} = D_{i,k_n}^{\text{eff}} + B_{i,\text{vis}}^{\text{eff}} = \frac{B_0}{\mu}\bar{p}_i + \frac{4}{3}K_0 v_M \quad (4)$$

The effective Knudsen diffusivity $D_{\text{i,k}_\text{n}}^{\text{eff}}$ is calculated from kinetic theory of gases as:[18]

$$D_{i,K_n}^{\text{eff}} = \frac{4}{3}K_0 v_M = 97r\frac{\varepsilon_s}{\tau}\sqrt{\frac{T}{M_i}} \quad (5)$$

For viscous flow, the momentum diffusion coefficient $B_{\text{i,vis}}^{\text{eff}}$ concerned with $\bar{p}_i$ the average pressure, μ viscosity of species i and B_0 morphological parameter in the support layer defined as:[19]

$$B_{i,\text{vis}}^{\text{eff}} = \frac{B_0}{\mu}\overline{p_i} = \frac{\varepsilon_{\text{vis}}}{\tau}\frac{d_0^2}{32\mu}\bar{p}_i \quad (6)$$

The average permeation flux can then be expressed in terms of the overall mass transfer coefficient:[20]

$$J_i = k_{i,\text{ov}}(C_{i,f} - p_{i,p}/H_i) \quad (7)$$

If sufficiently low total pressure is maintained on the permeate side, the permeate concentration may be considered negligible,[7] and then eq. (13) reduced to:

$$J_i = k_{i,\text{ov}}C_{i,f} \quad (8)$$

Equation (8) can be used to derive the overall transfer coefficient from the experimental measurements of flux J_i and feed concentration $C_{i,f}$.

EXPERIMENTAL

Membrane preparation

PDMS/PSF (membrane 1) composite membrane was kindly supplied by Dalian Institute of Chemical Physics. The PSF porous membrane was synthesized by means of Loeb-Sourirajan phase-inversion process, and was cast onto a nonwoven fabric. A PDMS coating solution consisting of two components (prepolymer 107 RTV and crosslinker) was poured over the surface of support and then dried at the ambient temperature. The thickness of top layer PDMS is 1 μm. PDMS/PA (membrane 2) membrane was prepared in our lab. The mixtures of polyamide and polysulfoneamide in a certain weight ratio were cast to form a flat microporous membrane by evaporation and then heat treatment. The porous membrane was dipped in *N*-methyl-pyrrolidane (NMP) solution, so that its micropores were tentatively clogged with NMP solution. A dilute PDMS solution was prepared by dissolving PDMS prepolymer (107RTV silicone rubber) and crosslinker (tetraethyl orthosilicate) in hexane. The PDMS solution was coated on surface of the microporous membrane and the polymerization was initialized *in situ* by a stannic compound, and then PDMS film formed. The membrane was further cured in a vacuum oven to form the final PDMS skin layer and NMP solution in the porous support layer is evaporated simultaneously. With this technique, PDMS polymer intruding into the porous support could be effectively avoided or minimized. The PDMS skin layer thickness can be determined by the amount of PDMS coating on the support surface. The estimation of the skin layer thickness is about 5 μm.

Scanning electron microscopy and energy dispersive spectroscopy

A scanning electron microscope (JEOL JMS-5910LV) was used to investigate the cross-sectional morphology of the composite PDMS membrane. The energy dispersive spectroscope (Oxford 7234) attached to the SEM was used to examine the chemical element distribution in the membranes. By means of EDS, a silicon concentration profile along the thickness of the composite membrane was determined by selecting the appropriate energy band. Point analyses could also be performed to get the local element contents.

Apparatus

The schematic experimental setup is given in Figure 2. A magnetic mixer and a temperature control were provided for the feed vessel (2-L in volume). The solution was fed into the membrane module at a given flow rate. The module was of a circular flat-plate design, providing 0.024 m^2 of membrane area. The retentate was circulated through the feed vessel and the module, while the permeate was collected in cold traps with refrigerant streams of −10 and −30°C, respectively. The downstream absolute pressure was kept at 10 mmHg in all experimental runs.

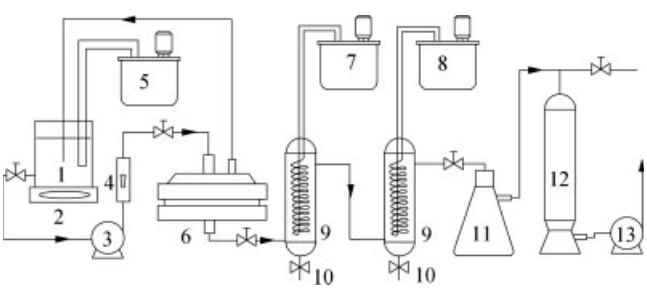

Figure 2 Schematic diagram of the experimental set-up for pervaporation. 1. feed vessel; 2. magnetic mixer; 3. pump; 4. rotameter; 5. thermostat; 6. membrane module; 7,8. refrigerator; 9. condenser; 10. sampling valve; 11. buffer tank; 12. desiccator; 13. vacuum pump.

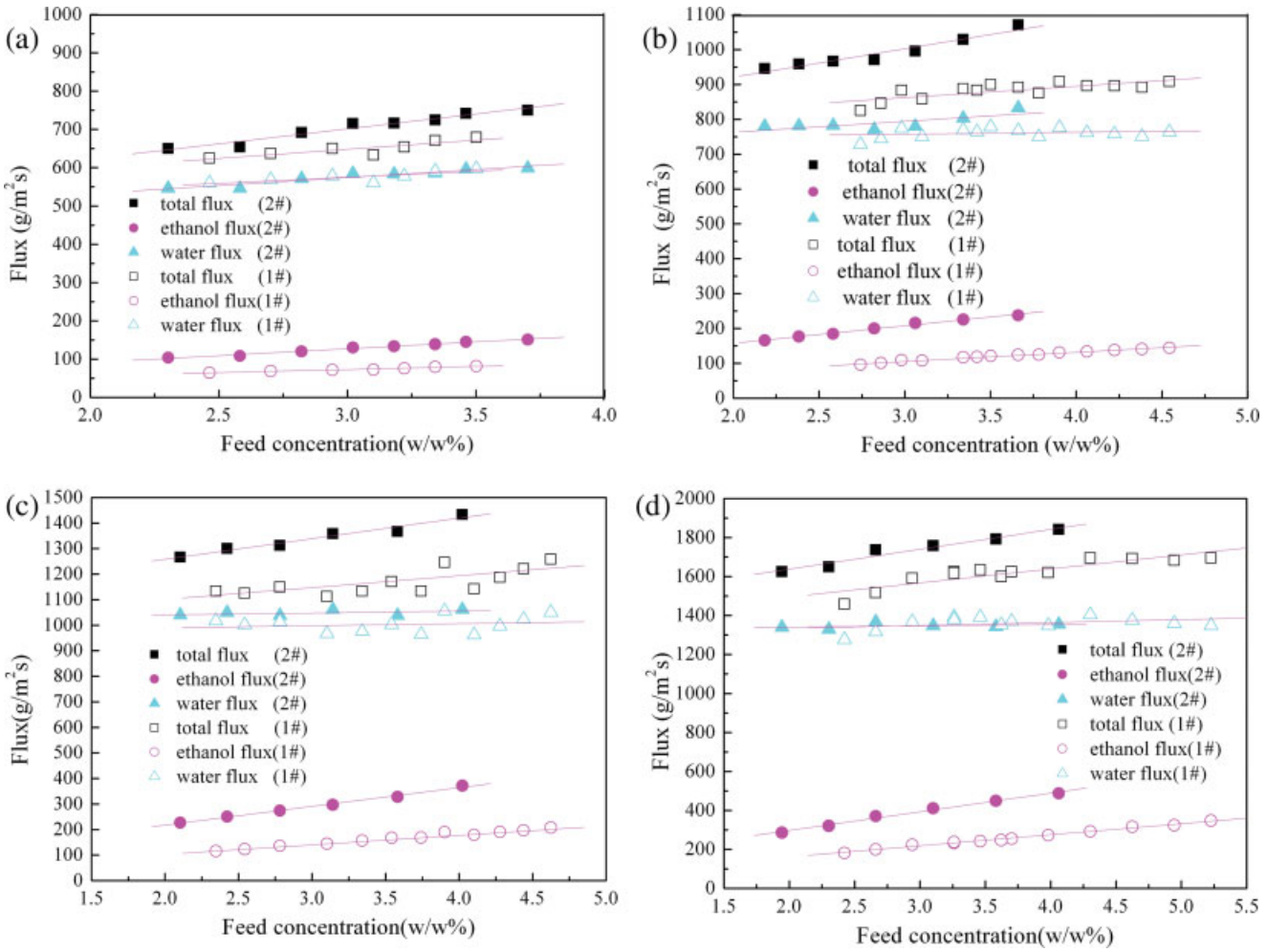

Figure 3 Dependence of pervaporation flux on concentration at different temperature. (a) Flux as a function of feed concentration at 30°C, (b) flux as a function of feed concentration at 35°C, (c) flux as a function of feed concentration at 40°C, (d) flux as a function of feed concentration at 45°C (1#, membrane 1; 2#, membrane 2). [Color figure can be viewed in the online issue, which is available at http://www.interscience.wiley.com.]

One series of experiments was performed under variable feed temperatures in the range of 303–318 K and fixed feed flow rate of 100 L/h. A densimeter (DMA4500, Anton Paar, Austria) was used to measure the organic concentration.

RESULTS AND DISCUSSION

Relationship between flux and operating variables

We determined the flux (J) as follows:

$$J = \frac{M}{At}$$

where M refers to weight of the permeate, A is the effective membrane area, t is the running time.

Figure 3 shows the dependence of pervaporation flux on feed concentration as a function of the operation temperature. Total permeate flux increases almost linearly with increasing ethanol concentration in the feed. The increasing is principally dominated by the increasing ethanol flux rather than water flux. The water flux remains relatively constant and independent of the ethanol concentration in the feed. Similar trend has been reported by Blume et al.[21] The total fluxes, ethanol fluxes, and water fluxes all increase monotonically with increasing temperature because the mobility of permeating molecules are enhanced by both the temperature and the higher mobility of the polymer segments. These results are consistent with those of previous studies.[22–25]

However, the ethanol fluxes across the PDMS/PA membrane were larger than those across the PDMS/PSF membrane at the same feed concentration and temperature. Taking the membrane thickness into consideration, specific permeation rate of membrane 2 was over membrane 1 by seven times at least. The reciprocal proportionality between transmembrane flux and membrane thickness has been leading an

effort to prepare ultra-thin membrane for a long time. However, it was observed through the experiments that a membrane with thinner active skin layer presented a permeation rate far smaller than a thicker membrane. In addition to the active layer thickness, there must be some factors influencing the permeation.

Relationship between separation factor and operating variables

Separation factor (α) is defined as following equation:

$$\alpha = \frac{Y_e/Y_w}{X_e/X_w}$$

where X_e and X_w are ethanol and water contents (wt %) in the feed, respectively, and Y_e and Y_w are ethanol and water content (wt %) in the permeate.

The evaluation of separation factor with operating parameters is shown in Figure 4. It could be observed that (1) the separation factors decreases slightly as the feed concentration rises; (2) the rise in temperature enhances the selectivity of ethanol to water; (3) the separation factor of membrane 2 is clearly higher than that of membrane 1.

For ethanol/water binary mixture, ethanol can interact more strongly with the membrane than water. The polarization of ethanol enables the membrane to be swollen more. Therefore, a small enlargement of the free volume will be allowed with increasing the feed concentration; the result is that ethanol can permeate easily through the membrane. But the concentration change of ethanol in the permeate is less than that of the feed. Thus, the separation factors decrease as shown in Figure 4. The effect of operating temperature on selectivity does not follow a simple relation because of complex temperature dependence of the polymer–solvent interaction parameter.[26] For ethanol–water mixture, some authors reported a decrease in the separation factors with temperature,[24,25] but others reported a reverse trend.[5,23] We have imaged that the increase of selectivity with temperature is possibly due to the apparent activation energy difference between water and ethanol because the ethanol molecule is larger than water molecule. The change of the ethanol permeate rate with the temperature is more violent than that of the water. Because the temperature change ratio gradually declines from 30 to 35°C, from 35 to 40°C, and from 40 to 45°C in turn, and diffusion and solubility of penetrating components in the membrane depend on the temperature, the gaps of separation factor resulted in by temperature would narrow with the decreasing temperature change ratio.

What is most concerned is the distinction on separation factor between two membranes. The ethanol/water selectivity of the PDMS/PSF is lower than that of the PDMS/PA membrane. This behavior is possibly due to the hydrophilicity of PSF material.

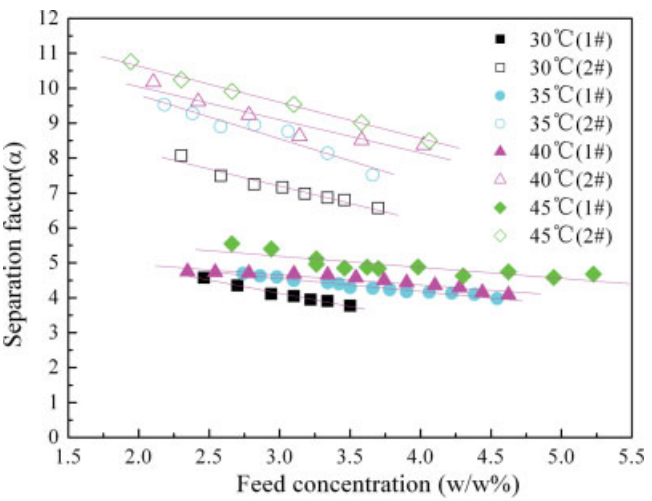

Figure 4 Dependence of separation factors on feed concentration at different temperature. [Color figure can be viewed in the online issue, which is available at http://www.interscience.wiley.com.]

Characteristics of the prepared flat-plate membranes

Figure 5 shows the cross section structures of the membranes investigated by SEM. The thickness of the PDMS active layer is about 1 μm for membrane 1 and 5 μm for membrane 2, seen from Figures 5(a–b). From Figure 5(a), the asymmetrical PSF support layer has a top skin layer of sponge-like structure with pores of nanometer magnitude and a sublayer of long finger-like holes with average diameter of around 8 μm. Figure 5(b) depicts the net-like support layer structure of membrane 2 with average diameter around 0.5 μm. In Figures 5(c–d), it was easily observed that the homogenous PDMS layers were dense. The binding interface between the top layer and support layer in the case of PA was relatively clear. However, in Figure 5(c), the interface was not clear in the case of PSF support layer, because the PDMS solution penetrated into pores of the PSF. This implies that an intermediate layer exists between PDMS top layer and PSF support. The layer should be a mixture of two polymers of PDMS and PSF.

SEM coupled technique, EDS allows a spectroscopic analysis of the elements in the membrane. A line was drawn in the middle of the SEM picture with PSF support, along which the Si signal was recorded with EDS as shown in Figure 6(a). Figure 6(b) shows the EDS spectra obtained in the same way from a PA support. The high peak on the right-side of graphs

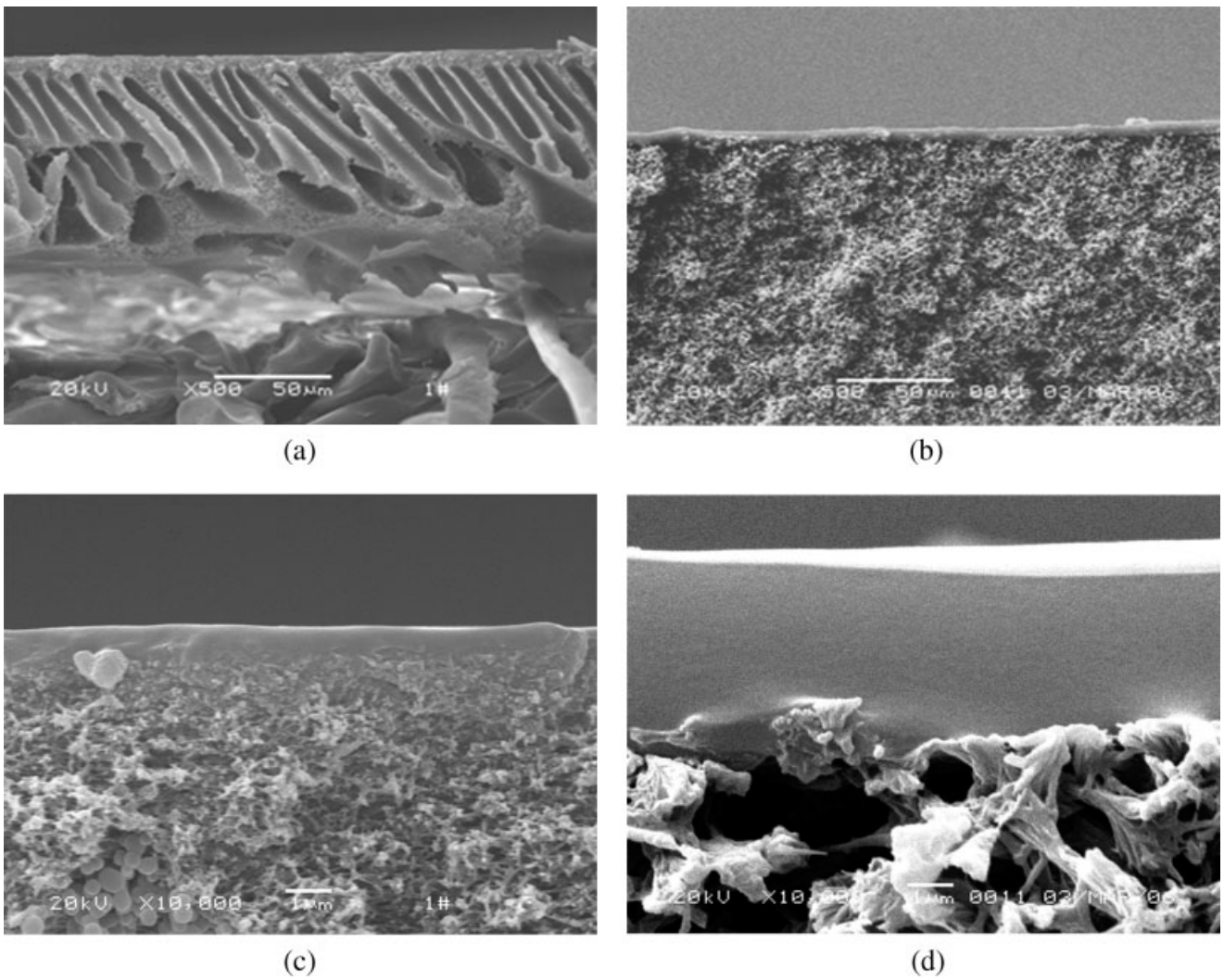

Figure 5 SEM photographs of two composite membranes: (a) PDMS/PSF (×500); (b) PDMS/PA (×500); (c) PDMS/PSF (×10,000); (d) PDMS/PA (×10,000).

corresponded to the high Si concentration in the top layer. The Si signal coming from the support layer could indicate the intrusion of PDMS in the support. Figure 6(a) proves that about 2 μm-thickness top layer polymer had intruded the support layer intensively. In the case of PA support, the distance of strong Si signal is about 5 μm, which demonstrated the PDMS polymer intruding into the porous support effectively minimized. The noise on the signals can be ascribed to instrument error and the uneven surface of the membrane cross section.

Analysis of permeation based on the resistance-in-series model

To determine the relative contribution of every resistance in the series transport process, we are quantitatively analyzing these resistances one by one.

The liquid film resistance was strongly dependent of hydraulic conditions in the membrane module and ethanol solution property (e.g., concentration and temperature). The similar hydraulic pattern and feed property should produce consistent film resistance. In accordance with usual concept, the transport resistance through top PDMS layer is directly proportional to membrane thickness and inversely proportional to average diffusivity and partition coefficient. Provided that both the material of top layer and properties of the feed solution are uniform, the partition coefficient S should be constant. Previous study[27] showed that the relative contribution of the top layer resistance was dominant, compared with that of the liquid film resistance at the feed flow rate of 100 L/h.

Because of the significant differences between support layer morphologies shown in Figure 5, it was considered necessary to investigate and isolate the influence of the membrane support layers upon component flux. In the case of a permeate pressure as low as 10 mmHg, where the average free path of

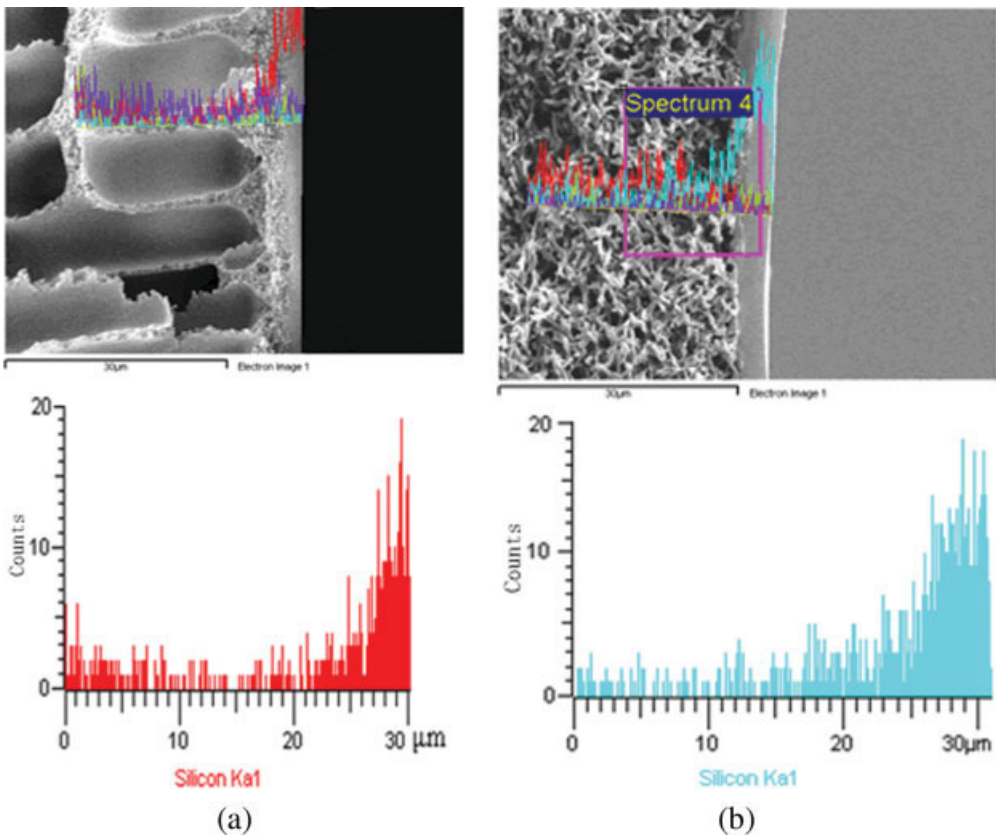

Figure 6 Si concentration pattern with EDS obtained on a cross section through (a) a PDMS/PSF and (b) a PDMS/PA composite membrane. [Color figure can be viewed in the online issue, which is available at http://www.interscience.wiley.com.]

vapor molecules was in the order of micrometer, the Knudsen number, $K_n = \lambda/2r$, determined vapor transport region because of the wide pore diameter distribution in the support layer.[28] In the spongy-like structure area of membrane 1, average pore diameter was about 20 nm. In the net-like structure of membrane 2, average pore diameter was about 0.5 µm. When the vapor transport was in the Knudsen region ($K_n \gg 1$), and then the Knudsen diffusion effect was more important than viscous flow. The effective Knudsen diffusivity $D^{\text{eff}}_{\text{k,n,i}}$ was calculated by eq. (5) at 30–45°C, and some intermediate parameters were estimated reasonably for material involved. In the finger-like structure area of membrane 1, average pore diameter was about several micrometers. The pore size was much larger than the mean free path of the molecules and viscous flow dominated. The momentum diffusion coefficient $B^{\text{eff}}_{\text{vis,i}}$ was calculated by eq. (6).

The transport through the support layer of membrane 1 was mainly governed by Knudsen diffusion and viscous flow, while the transport through the support layer of membrane 2 was controlled by Knudsen diffusion. Some important parameters, calculated at 10 mmHg permeate pressure, are presented in Table I. According to eq. (4), the minimal equivalent diffusion coefficient $D_{i,v}$ of support layer of two membranes were in the order of 10^{-7} and 10^{-4}. Many literatures have reported diffusivity for ethanol in silicone rubber membrane. Watson and Payne[29] reported that the diffusivity in PDMS membrane was 7×10^{-10} m^2/s for the solution 1% by volume ethanol in water at 80°C. LaPack et al.[30] measured experimentally diffusivity for a variety of substance in PDMS membrane filled with fumed silica, and the diffusivity was 0.4×10^{-10} m^2/s obtained for ethanol corresponding to feed concentration of 0.1 wt % and temperature of 25°C. Diog et al.[31] gave diffusivity for ethanol in PDMS membrane of 6×10^{-10} m^2/s at feed temperature of 25°C, while ethanol diffusivities obtained from Chandak et al.[32] in PDMS at 25°C and 100°C were 1.52×10^{-10} and 1.57×10^{-10} m^2/s, respectively. From the literature data, the diffusivity of ethanol in PDMS membrane has an order of magnitude 10^{-10} m^2/s at wide range of temperature. Calculation for porous layer of support layer indicated that the effective diffusivity was three orders of magnitude higher than the diffusivity in the dense PDMS layer presented in the literatures.

Considering the thickness of the top layer and support layer, the top layer resistances δ/P of two mem-

TABLE I
Diffusion Coefficient Data of Porous Support Layer for Organic Permeating Component

Composite membrane	Support layer	$\delta_{support}$ (μm)	d_0 (μm)[a]	ε [a]	r[b]	p_p (Pa)	T (°C)	$D^{eff}_{k_{n,i}}$ (m^2/s)	$B^{eff}_{vis,i}$ (10^{-4} m^2/s)
PDMS/PSF	PSF	5/80[c]	0.02/8[c]	0.15/0.5	1	1,333	30	7.469×10^{-7}	1.362
					1	1,333	35	7.530×10^{-7}	1.339
					1	1,333	40	7.591×10^{-7}	1.329
					1	1,333	45	7.651×10^{-7}	1.294
PDMS/PA	PA	120	0.5	0.7	1	1,333	30	8.713×10^{-5}	
					1	1,333	35	8.785×10^{-5}	
					1	1,333	40	8.856×10^{-5}	
					1	1,333	45	8.925×10^{-5}	

[a] The porosity and the pore diameter of the support material were obtained from the SEM and the literature.
[b] The porous support is assumed to a bundle of straight cylindrical capillaries.
[c] The top skin layer with little pores/sublayer with larger pores.

branes were over two orders of magnitude higher than the support resistances δ_v/D_v. Compared with the PDMS top layer resistance, the porous support layer resistances can be ignored.

According to above-mentioned analysis, it seems that the overall resistance for the composite membranes should be attributed to the dense top PDMS layer. Although the prepared conditions for two membranes are slightly different, EDS analysis showed the content of C, O, Si in two PDMS top layer is about the same, presented in Table II. The permeability of PDMS top layer is reasonably assumed to be same.

We are put into a serious puzzle. The ratio of membrane thickness of membrane 2 to membrane 1 is equal to 5, and thus the ratio of the ethanol fluxes should be one-fifth according to eqs. (1) and (8), but the experimental result is over 1.5 (Fig. 3). Estimates of the permeability of the organic component can be obtained from eqs. (1) and (8) and the above-mentioned analysis. The values of P of PDMS material for ethanol are 0.683×10^{-12} and 5.96×10^{-12} m^2/s for membrane 1 and membrane 2 corresponding to feed concentration of 3 wt % and temperature of 30°C. Gudernatsch et al.[16] obtained an equation to determine the top layer PDMS permeability and we calculated the value of 7.81×10^{-12} m^2/s at the same feed condition. The top layer permeability of PDMS/PA membrane is reasonably agree with the literature value, but the value of PDMS/PSF membrane is about 10 times lower than that of PDMS/PA and literature value. Analyzing using conventional concept and theory, we cannot find the reason for these contradictive results.

The SEM pictures indicate that there are not absolutely clear interfaces between the PDMS layer and the PSF or PA support layer (Fig. 5). The intrusion of PDMS into the porous PSF supports is around 2 μm in depth (Fig. 6). This must increase the resistance to some extent. According to earlier method,[12,13,16] the resistance of binding interface is considered as parallel-resistance model and was calculated by eq. (3). Because PSF is water-selective and yet PDMS is ethanol-selective, the permeation resistance of PSF is beyond that of PDMS at same feed condition. Parallel-resistance is smaller than either of the two resistances. So the overall resistance of binding interface is equal to the PDMS resistance at most. If we deal with the binding interface as a portion of PDMS top layer, the PDMS layer thickness of membrane 1 is only three-fifths of that of membrane 2, even if adding 2 μm intrusion depth. The flux of membrane 1 should be one and two-thirds times of the membrane 2. It is similarly contradictory with the experimental results (two-third times). So it can be imaged that PDMS penetrating PSF produced larger resistance than its intruding PA and also beyond the intrinsic PDMS resistance. Otherwise we cannot explain the large gap of permeation performance between membrane 1 and membrane 2. We wonder why the intrusion layer of only 2 μm gives so significant effect on the separation performance. Perhaps, interaction of the two materials in the binding layer caused some changes on structures?

Furthermore, based on the result of the experiments and the analysis, the resistance of the binding interface cannot simply be replaced by the top layer. This may lead a new definition on the transport resistance through a multilayer composite membrane with a dense PDMS top layer.

TABLE II
EDS Analysis of C/O/Si Ratios at Cross Sections of PDMS Top Layer

	PDMS/PSF		PDMS/PA	
Element	wt %	Atomic %	wt %	Atomic %
C	48.60	64.43	47.49	63.41
O	15.02	14.95	15.34	15.37
Si	36.37	20.62	37.17	21.22

CONCLUSIONS

A composite PDMS-PA membrane was prepared by a solvent-clogging method to separate ethanol from water. The prepared membrane and a commercial composite PDMS-PSF membrane were investigated contrastively for their permeation performance in pervaporation. It was found that the specific permeate rate of PDMS-PA membrane (numbered 2) was over PDMS-PSF membrane (numbered 1) by seven times at least, with taking the membrane thickness into consideration.

The quantitative analysis for the series resistances in the membranes has been carried out to probe into their mass transfer. It showed that the overall resistance of the composite membranes should be attributed to the dense top PDMS layer; calculation for support layer indicated that the minimal effective equivalent diffusivity, independent of the support layer material, was three orders of magnitude higher than the diffusivity in the dense PDMS layer presented in the literatures.

Analyzing using conventional concept and theory, we cannot find the reason for these contradictive results that the ratio of membrane thickness of membrane 2 to membrane 1 is equal to 5, but the ratio of the ethanol fluxes experimentally is over 1.5 (Fig. 3). From the SEM pictures and EDS for chemical element distribution along membrane thickness, intrusion of the dense polymer in the PSF support pores is more severe than that of the PDMS/PS membrane, and the focus concentrated on the binding interface between the active layer and support layers. We wonder why the intrusion layer of only 2 μm gives so significant effect on the separation performance. Perhaps interaction of the two materials in the binding layer caused some changes on structures? This may lead a new definition on the transport resistance through a multilayer composite membrane with intrusion of dense PDMS top layer. More studies are currently under investigation.

NOMENCLATURE

Symbol definition

A	effective membrane area (m^2)
B_0	morphological parameter (m^2)
$B^{\text{eff}}_{\text{vis,i}}$	momentum diffusion coefficient (m^2/s)
C_f	feed concentration in bulk feed solution (kg/m^3)
d_0	the diameter of porous in support layer of membrane (m)
$D^{\text{eff}}_{\text{k}_{\text{n,i}}}$	effective Knudsen diffusion coefficient of component i in support layer (m^2/s)
$D_{i,v}$	equivalent diffusion coefficient of component i through support layer
H	membrane/aqueous phase partition coefficient
J_i	permeation flux of component i (mol/m^2 s or kg/m^2 s)
k_l	liquid film mass transfer coefficient (m/s)
k_{ov}	total mass transfer coefficient (m/s)
K_0	morphological parameter (m^2)
K_n	Knudsen number, dimensionless
M_i	molecular mass of component i (kg/kmol)
M	the weight of the permeate (kg)
$p_{i,p}$	the partial pressure in the permeate (Pa)
$\overline{p_i}$	mean pressure inside the porous medium (Pa)
P	liquid permeability of dense layer
P_{binding}	liquid permeability of binding interface
P_m	liquid permeability PDMS top layer
P_{support}	liquid permeability support material
r	radius of porous in support layer of membrane (m)
t	given pervaporation time (s)
T	temperature on upstream and downstream of the membrane (T)
X_e	weight fractions of ethanol in the feed
X_w	weight fractions of ethanol in the feed
Y_e	weight fractions of ethanol in the permeate
Y_w	weight fractions of water in the permeate
v_M	mean molecular speed $= \sqrt{(8RT/\pi M)}$

Greek letters

α	separation factor
δ	dense layer thickness (m)
δ_{binding}	binding interface thickness (m)
δ_m	top layer membrane thickness (m)
δ_v	support layer thickness of membrane (m)
μ	dynamic viscosity (Pa s)
ε_s	porosity of the skin layer of porous support, dimensionless
ε_{vis}	porosity of the sublayer of porous support, dimensionless
λ	mean free path in the support layer (m)
τ	tortuosity of the support layer of the membrane, dimensionless

References

1. Takegami, S.; Yamada, H.; Tsujii S. J Membr Sci 1992, 75, 93.
2. Wang, X. P.; Feng, Y. F.; Shen, Z. Q. J Appl Polym Sci 2000, 75, 740.
3. Kimura, S.; Nomura, T. Membrane 1982, 7, 352.
4. Mohammadi, T.; Aroujalian, A.; Bakhshi, A. Chem Eng Sci 2005, 60, 1875.
5. Liang, L.; Ruckenstein, E. J Membr Sci 1996, 114, 227.
6. Lau, W. W. Y.; Finlayson, J.; Dickson, J. M.; Jiang, J. X.; Brook, M. A. J Membr Sci 1997, 134, 209.
7. Bode, E.; Busse, M.; Ruthenberg, K. J Membr Sci 1993, 77, 69.
8. Li, L.; Xiao, Z. Y.; Tan, S.; Pu, L.; Zhang, Z. J Membr Sci 2004, 243, 177.
9. Vankelecom, I. F. J.; Moermans, B.; Verschueren, G.; Jacobs, P. A. J Membr Sci 1999, 158, 289.
10. Hong, Y. K.; Hong, W. H. J Membr Sci 1999, 159, 29.

11. Satyanarayana, S. V.; Sharma, A.; Bhattacharya, P. K. J Membr Sci 2004, 102, 171.
12. Henis, J. M. S.; Tripodi, M. K. J Membr Sci 1981, 8, 233.
13. Lipnizki, F.; Olsson, J.; Wu, P.; Weis, A.; Tragårdh, G.; Field, R. W. Sep Sci Technol 2002, 37, 1747.
14. Liu, M. G.; Dickson, J. M.; Côté, P. J Membr Sci 1996, 111, 227.
15. Nakagawa, T. In Membrane Science and Technology; Osada, Y., Nakagawa, T., Eds.; Marcel Dekker: New York, 1992; pp 239–287.
16. Gudernatsch, W.; Menzel, Th.; Strathmann, H. J Membr Sci 1991, 61, 19.
17. Beuscher, U.; Gooding, C. H. J Membr Sci 1997, 132, 213.
18. Cunningham, R. E.; Williams, R. J. J. Diffusion in Gases and Porous Media; Plenum Press: New York, 1980.
19. Altena, F. W.; Bargeman, D.; Smolders, C. A.; Knoef, H. A. M.; Heskamp, H. J Membr Sci 1983, 12, 313.
20. Wijmans, J. G.; Baker, R. W. J Membr Sci 1995, 107, 1.
21. Blume, I.; Wijmans, J. G.; Baber, R. W. J Membr Sci 1990, 49, 253.
22. Lipski, C.; Côté, P. Environ Prog 1990, 9, 254.
23. Li, X. H.; Wang, S. C. Sep Sci Technol 1996, 31, 2867.
24. Vankelecom, I. F. J.; Depre, D.; Beukelaer, S. D.; Uytterhoeven, J. B. J Phys Chem 1995, 99, 13193.
25. te Hennepe, H. J. C.; Bargeman, D.; Mulder, M. H. V.; Smolers, C. A. J Membr Sci 1987, 35, 39.
26. Dutta, B. K.; Ji, W.; Sikdar, S. K. Sep Purif Method 1997, 25, 131.
27. Li, L.; Xiao, Z. Y.; Zhang, Z. B.; Tan, S. J. J Chem Ind Eng 2002, 53, 1169 (in Chinese).
28. Zhdanov, V. M. Adv Colloid Interface 1996, 66, 1.
29. Watson, J. M.; Payne, P. A. J Membr Sci 1990, 49, 171.
30. LaPack, M. A.; Tou, J. C.; McGuffin, V. L.; Enke, C. G. J Membr Sci 1994, 86, 263.
31. Diog, S. G.; Boam, A. T.; Livingston, A. G.; Stuckey, D. C. J Membr Sci 1999, 154, 127.
32. Chandak, M. V.; Lin, Y. S.; Ji, W.; Higgins, R. J. J Appl Polym Sci 1998, 67, 165.